

Article

Fuel Consumption and CO₂ Emission Reductions of Ships Powered by a Fuel-Cell-Based Hybrid Power Source

Gilltae Roh ¹, Hansung Kim ¹, Hyeonmin Jeon ²  and Kyoungkuk Yoon ^{3,*} 

¹ Department of Chemical and Biomolecular Engineering, Yonsei University, 134 Shinchon-dong, Seodaemun-gu, Seoul 120-749, Korea

² Department of Marine System Engineering, Korea Maritime and Ocean University, 727 Taejong-ro, Busan 49112, Korea

³ Department of Electrical Engineering, Colleges of Korea Polytechnic, 155 Sanjeon-ro, Ulsan 44482, Korea

* Correspondence: kkyoon70@kopo.ac.kr; Tel.: +82-(0)1055410424

Received: 17 May 2019; Accepted: 15 July 2019; Published: 18 July 2019



Abstract: The need for technological development to reduce the impact of air pollution caused by ships has been strongly emphasized by many authorities, including the International Maritime Organization (IMO). This has encouraged research to develop an electric propulsion system using hydrogen fuel with the aim of reducing emissions from ships. This paper describes the test bed we constructed to compare our electric propulsion system with existing power sources. Our system uses hybrid power and a diesel engine generator with a combined capacity of 180 kW. To utilize scale-down methodology, the linear interpolation method is applied. The proposed hybrid power source consists of a molten carbonate fuel cell (MCFC), a battery, and a diesel generator, the capacities of which are 100 kW, 30 Kw, and 50 kW, respectively. The experiments we conducted on the test bed were based on the outcome of an analysis of the electrical power consumed in each operating mode considering different types of merchant ships employed in practice. The output, fuel consumption, and CO₂ emission reduction rates of the hybrid and conventional power sources were compared based on the load scenarios created for each type of ship. The CO₂ emissions of the hybrid system was compared with the case of the diesel generator alone operation for each load scenario, with an average of 70%~74%. This analysis confirmed the effectiveness of using a ship with a fuel-cell-based hybrid power source.

Keywords: hybrid power source; fuel cell; molten carbonate fuel cell (MCFC); carbon dioxide; electric propulsion system

1. Introduction

In 2015, the “Third IMO Greenhouse Gas Study,” conducted by the International Maritime Organization (IMO) [1], reported that air pollutants emitted from ships in 2012 accounted for 13% of NO_x, 12% of SO_x, and 2.6% of CO₂ in terms of global atmospheric pollutant emissions [2,3]. The International Council on Clean Transport (ICCT), an international environmental non-profit organization, has analyzed and forecasted the pollutant emissions from ships from 1990 to 2050, and reported that the NO_x and SO_x emitted from ships are expected to increase to 30% and 20%, respectively, of all global pollutant emissions [3–5]. These study results support the view that the long-term effects of atmospheric pollutants caused by ships are foreseen to become more severe, considering the trend of increasing global trade in the future. Clearly, there is a need to develop technology for reducing pollutant emissions from ships [6,7].

Currently, fuel cells that use hydrogen fuel to reduce pollutant emissions from ships are being studied [8–11]. Fuel cells take the chemical energy within the hydrogen that is used as fuel and convert it into electrical and thermal energy through an electrochemical reaction with the oxygen present in the air. They produce almost no pollutant emissions or noise when generating electricity, and they can use various fuels as sources of hydrogen. Fuel cells are an eco-friendly energy source with very high electrical efficiency. Fuel-cell-based power generation can reduce greenhouse gas emissions by 30% compared to existing power generation methods [12]. Therefore, most advanced countries throughout the world regard fuel cells as a next-generation technology and are actively developing them [13,14].

The research on a hybrid system combining a fuel cell system with a diesel engine, which is the main power source of a ship, has been conducted in Europe [15–18]. The report of the European Maritime Safety Agency (EMSA), ‘Study on the Use of Fuel Cells in Shipping’, applied fuel cells as the main power or auxiliary power of ships from the beginning of 2000 and 24 projects in Europe and the United States with the beginning of the ‘US Ship Service Fuel Cell Program [US SSFC]’ project [19]. Analysis of these studies shows that most of the methods are generally aimed at improving the performance of hybrid systems (fuel cells, diesel generators) or the configuration of their systems and that there is no experimental study on the reduction of CO₂ emissions from the hybrid power generation systems [20,21].

Therefore, an empirical study was conducted through experiments on CO₂ reduction that has not been carried out in previous projects so far. Molten carbonate fuel cells (MCFCs) were selected as fuel cell systems of a combined power source because the characteristics of MCFCs are suitable for application to ships [22,23]. Since MCFCs operate at high temperature, the reaction rate is fast, even when using low-cost catalysts, as compared with relatively different fuel cell systems. Even when the ship is sailing for a long time, the external reformer is not installed separately and natural gas or coal gas is directly used as fuel. It is appropriate to apply it as the main power source for the base load of the ship [24].

In this study, to reduce the emissions from ships, empirical experiments on the fuel consumption and carbon dioxide emission reduction effect of a combined power source (fuel cell + battery + diesel generator) instead of the diesel generator were conducted. The capacity of the combined power source was 100 kW for MCFCs, 30 kW for batteries, and 50 kW for diesel generators. In order to carry out the experiment on the test bed, the power amount for each operation mode was analyzed according to the type of the commercial vessel, and the scale was downsized according to the capacity of the test bed. The fuel consumption and carbon dioxide emissions of the ship were calculated, according to the load profile of the ship, within 180 kW of the configured system. It can be confirmed through the demonstration that carbon dioxide emission and fuel consumption was considerably reduced compared to the conventional diesel power source.

2. Background

The International Convention for the Prevention of Marine Pollution from Ships (MARPOL) agreed that emissions, such as NO_x and SO_x, from ships should be reduced by 20% or less of the current emission amounts from 2008 to 2015. Since 2016, the agreement has recommended an 80% reduction in pollutant emissions [25]. In addition, the IMO has introduced the energy efficiency design index (EEDI), which is an index of factors to be considered in ship design to contribute toward reducing CO₂ emissions. The CO₂ emission regulations based on the EEDI that were imposed by the IMO on all new ships built since 2013 are listed in Tables 1 and 2. Ships that do not meet the required EEDI levels are prohibited from entering ports [26]. In Table 2, the EEDI will be implemented in phases. Currently, it is in phase 1, which runs from year 2015 to 2019. Phase 2 will run from year 2020 to 2024 and phase 3 from year 2025 onwards [27].

Table 1. International Convention for the Prevention of Marine Pollution from Ships (MARPOL) 73/78—Annex VI Regulations for the Prevention of Air Pollution from Ships.

| Year Built | Capacity | NO _x | SO _x | PM | Remarks |
|------------|----------|-----------------|-----------------|------------|--------------|
| 2008~2015 | >125 kW | 7.7 g/kWh | 24 kg/ton | 1.2 kg/ton | 20% decrease |
| 2016~ | | 2.0 g/kWh | 6 kg/ton | 0.3 kg/ton | 80% decrease |

Table 2. The energy efficiency design index (EEDI)-based CO₂ emission reduction goals.

| Phase 0 (Year Built) | Phase 1 | Phase 2 | Phase 3 |
|---------------------------------------|---------------------------|---------------------------|-----------------------|
| 2013~2014 Scheduled to take effect | 2015~2019 10% decrease | 2020~2024 20% decrease | 2025~ 30% decrease |

National and international regulations are gradually being strengthened and require ocean pollutant emissions from ships to be reduced continuously. However, it is not possible to address this problem solely through modern engine technology without installing additional devices for preventing environmental pollution. Therefore, there is an increasing demand for high-efficiency power sources for ships with almost no pollutant emissions. Normal high-efficiency diesel engines have an energy efficiency of approximately 40%, and facilities equipped with CO₂-capturing devices or pollutant-processing devices for emission gases have limited effectiveness owing to increases in the system volume and fuel energy consumption [28].

On the other hand, if fuel cells powered by hydrogen, which are eco-friendly high-efficiency power sources, could be an alternative solution, instead of diesel engines, to a propel ship, there could be almost no emissions (for example, NO_x, SO_x, CO₂, or PM); the fuel cells would produce no noise or vibration and would have good power generation efficiency [14]. As such, fuel cells powered by hydrogen have considerable potential as a next-generation main power source for ships. In addition, they can be modularized to reduce complexities in terms of their construction and installation. Therefore, their capacity can be adjusted such that it is most effective for specific types or functions of ships. They have a very wide range of uses and are considered a technology that will play a leading role in ship propulsion systems in the future [8,29].

3. Types and Properties of Fuel Cell Systems

Most fuel cells generate electricity and heat via the chemical reaction between hydrogen and oxygen, and water is created as the product. Various types of fuel cells are being studied, and each of these fuel cells is classified according to the characteristics of its electrolyte. The properties of these cells are described in Figure 1 and Table 3 [19,24].

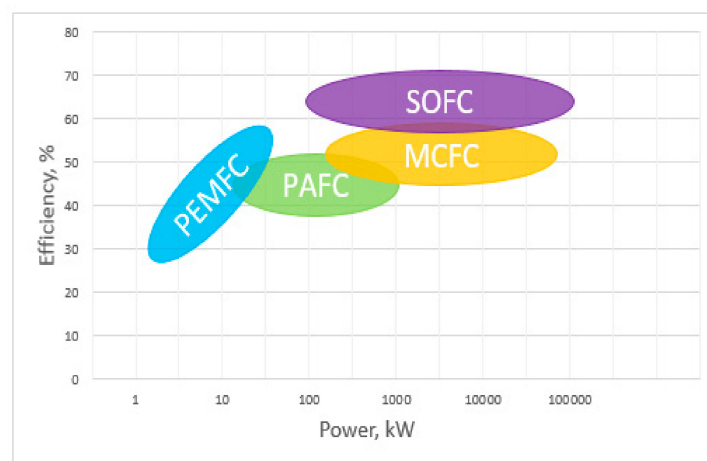


Figure 1. Comparison of efficiency versus power generation in each type of fuel cell.

Table 3. Fuel cell types (catalyst, durability, and hydrogen storage).

| Fuel Cell Types | Main Fuel | Electrolyte | Temperature of Generation | Level of Technology | Subject of Application |
|-----------------|-------------------------|-----------------------------|-----------------------------|-------------------------------------|--------------------------------|
| PEMFC | Hydrogen Methanol | Ion conductive polymer film | Ordinary temperature~100 °C | Development and demonstration phase | Small power source, Automobile |
| MCFC | Natural gas Coal gas | Molten carbonate | 600~700 °C | Development phase | Hybrid power generation |
| PAFC | Natural gas Methanol | Phosphoric acid | 150~200 °C | Commercialization phase | Distributed power system |
| SOFC | Natural gas Coal gas | Solid oxide | 700~1000 °C | Development phase | Hybrid power generation |
| AFC | Hydrogen | Potassium hydroxide | 80~120 °C | Commercialization phase | Space missions |

Although there are various types of fuel cells, such as in Table 3, in this paper, MCFCs are considered to be the main power source for the base load of the ship and were applied on the test bed. Because MCFCs operate at a high temperature, they can achieve a fast reaction rate even with a comparatively low-cost catalyst, a simple system design of a fuel cell, and low initial investment cost. In addition, even when the ship is sailing for a long time, natural gas or coal gas can be directly used as a fuel without installing an external reformer separately [16,22,23].

4. Comparative Analysis of Fuel Consumption and CO₂ Emission Reductions in Hybrid Power Sources vs. Conventional Commercial Diesel Generators

4.1. Greenhouse Gas Calculation Method

4.1.1. Intergovernmental Panel on Climate Change (IPCC) Emission Coefficient

Emissions from ships include greenhouse gases (GHGs) emitted from the diesel engines, steam engines with boilers, and gas turbines, which are the main engine types used to power ships, ranging from leisure crafts to large-scale freighters. The emitting crafts, which are the focus of the ship section of the “Intergovernmental Panel on Climate Change (IPCC) Guidelines 2006” report, include sailing ships, fishing boats, and other ships. The method for calculating GHG emissions is presented in Table 4 [30].

Table 4. Calculation methods according to emission gas.

| | CO ₂ | CH ₄ | N ₂ O |
|----------------------|-----------------|-----------------|------------------|
| Estimate methodology | Tier 1,2 | Tier 1,2 | Tier 1,2 |

The activity data used in the Tier 1 method are based on fuel consumption, thus emission coefficients are needed for each fuel and pollutant. In the case of CO₂, SO₂, and heavy metals, there is a close relationship between the emission coefficient and the CO₂, SO₂, and heavy metal content of the fuels. The calculations must take into account the related pollutant content in the fuel for each year and the target class of the ship according to the national region.

Tier 1 and Tier 2 emissions were calculated by using a method that uses petroleum sales as the index for the basic level of activity. It performs calculations by assuming the averaged characteristics of each ship type. The method to calculate Tier 3 emissions was based on the operating profile information of the ship. The Tier 3 method can be used when it is possible to collect not only the data on the engine, fuel usage, and duty cycle of the ship, but also information about its voyage. Because the actual voyage data of the ship must be taken into account, port arrival/departure statistical data regarding the voyage of the ship was used to calculate the fuel consumption and emissions while taking into account the

emissions for each operating profile and the ship type, fuel type, engine type, technical specifications, and engine load, yearly operating time, etc.

4.1.2. IMO Conversion Emission Factor

At the 1997 MARPOL conference, research on the GHGs emitted by ships was presented via a discussion on “CO₂ emissions from ships.” The first GHG study performed by the IMO was presented at the 45th the Marine Environment Protection Committee [MEPC] conference. At the 56th MPEC conference, it was determined that a second IMO GHG study would be performed to examine atmospheric emissions caused by exhaust gas emissions, volatile fuel emissions, and refrigerant leaks.

One goal of this study is to calculate the CO₂ emissions occurring when a hybrid power source is used in a ship. For this, only the exhaust gas emissions of the diesel engine and fuel cell were considered. Although the IPCC calculates GHG emissions by taking into account the ship type, fuel type, engine type, etc., this study used the CO₂ mass conversion factor, a dimensionless constant, presented in the “Calculation of Energy Efficiency Operational Indicator Based on Operational Data” to calculate the CO₂ emissions (IMO MEPC1/Circ 684 2009). GHG emissions were calculated by using the IPCC 2006 guidelines for CH₄ and N₂O in Table 5 (IPCC 2006), and the ISO 8217 Grades DMX conversion factor was used for CO₂ [31–33].

Table 5. Fuel-based exhaust gas emission factors.

| Emission | Emission Factor | Guideline Reference |
|------------------|----------------------------|---------------------|
| CH ₄ | 0.3 [$T_{CH_4}/TFuel$] | IPCC 2006 |
| N ₂ O | 0.08 [$T_{N_2O}/TFuel$] | IPCC 2006 |
| CO ₂ | 3.206 [$T_{CO_2}/TFuel$] | ISO 8217 Grades DMX |

4.2. Specifications of Components in the Fuel-Cell-Based Hybrid Power Source Test Bed

The process flow diagram (PFD) of the fuel-cell-based hybrid power source test bed is shown in Figure 2. The test bed was composed of the following specific components: The MCFC system, energy storage system (ESS), diesel generator, load bank, and intelligent energy management system [34–37].

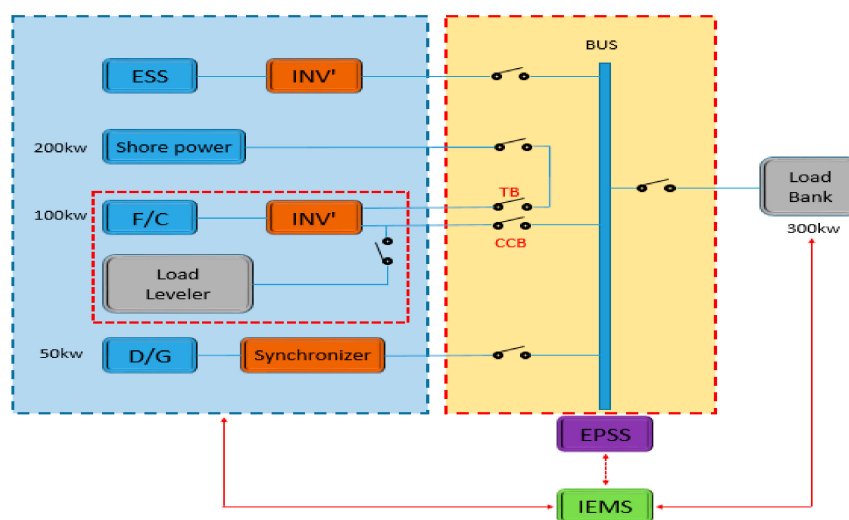


Figure 2. Process flow diagram of the test bed.

4.2.1. MCFC System

The fuel cell used in the test bed was a 300 kW MCFC system composed of a stack module, an electric balance of plant (EBOP), and a machinery balance of plant (MBOP) [38]. The fuel cell system constituting the combined power source was operated with a rated capacity of 300 kW. However,

a 100 kW output was used in a practical test bed. The MBOP was pretreated to make a better chemical reaction between the fuel gas and air, which concludes a pre-former, heater, humidifier, valves, pump, and blower [39]. The specifications are listed in Table 6.

Table 6. DFC300 MA system specifications.

| DFC300 MA Generation Plant Specifications | |
|---|--------------|
| Machinery Balance of Plant [MBOP] | |
| Height (Main enclosure) | 9.6' |
| Height (Ship loose items) | 14.6' |
| Width | 8.0' |
| Length | 19.8' |
| Weight | 12,292 kg |
| Electric Balance of Plant [EBOP] | |
| Height | 9.5' |
| Width | 3.5' |
| Length | 9.0' |
| Weight | 12,292 kg |
| Stack Module | 8.4' |
| Height | 8.2' |
| Width | 15.0' |
| Length | 18,143 kg |
| Total Weight | 42,727 kg |
| Power output | |
| Rated output | 250 kW |
| Voltage | 380~480 VAC |
| Frequency | 50~60 Hz |
| Power quality | Per IEEE 519 |

The peripheral equipment needed by the fuel cell system is shown in Figure 3. It includes a fuel injection part for supplying natural gas, a potable water injection part for producing ultrapure water, a part for emitting drainage water resulting from the production of ultrapure water, and a nitrogen/mixed gas injection part for protecting the stack. The air injection and exhaust gas emission parts were at the top of the MBOP. Two exhaust fans were installed within the MBOP [40].

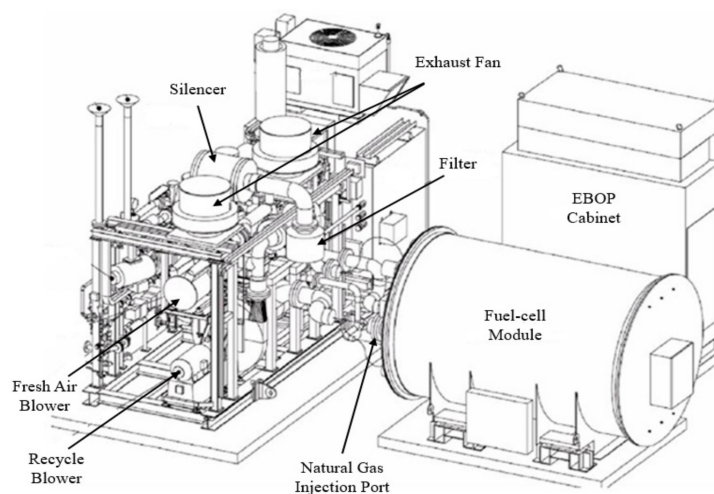


Figure 3. Configuration diagram of peripheral equipment for DFC300 MA.

The power generation concept of the fuel cell system is shown in Figure 4. The system was composed of a heat-up operating mode, which increases the initial temperature of the fuel cell stack

Table 7. ESS general battery and inverter specifications.

| Division | | Item | Specification |
|----------|--------------------------------|---------------------------------|---|
| Battery | General | Rated output | 100 kW |
| | | Rated voltage | 407 VDC |
| | | Capacity | 300 AH |
| | | Assembly of Cell | 110S/2P |
| | | Range of voltage | 352 V~451 V |
| | | Max discharge current | 600 A |
| | | Protection Communication | OVP, UVP, OCP, OTP RS 232C, CAN 2.0 |
| Inverter | Alternating Current [AC] Input | Composition | 3 Phase |
| | | Voltage | 440 VAC |
| | | Frequency | 50/60 Hz |
| | | Rated output | 100 kW |
| | Output | Total Harmonic Distortion [THD] | Below 5% |
| | | Voltage | 440 VAC |
| | | Frequency | 50/60 Hz |
| | Function | Rated output | 100 kW |
| | | Protection | Over current, Over temperature, Over voltage, Low battery shutdown, Reverse flow |

4.2.3. Diesel Generator System (DGS)

The 50 kW synchronous generator used in the test bed is a revolving-field-type generator which uses a permanent magnet. Its specifications are given in Table 8.

Table 8. Hybrid test bed and generator specifications.

| Item | | Specification |
|----------------|----------------------|------------------------|
| Engine part | Standby power rating | >95 PS |
| | Engine type | 4 Stroke, Water cooled |
| | Revolution | 1800 rpm |
| | Number of cylinders | 6 |
| | Cylinder type | Vertical series |
| | Governor type | Speed control type |
| | Cooling system | Radiator type |
| | Fuel | Diesel |
| | Starting system | DC 24 V battery start |
| Generator part | Type | Revolving field magnet |
| | Standby power rating | 50 kW/62.5 kVA |
| | Prime power rating | 45 kW/56 kVA |
| | Voltage | 440/254 V |
| | Current | 82 A |
| | Phase and wire | Three phase four wire |
| | Frequency | 60 Hz |
| | Power factor | 0.8 Lag |
| | Pole | 4 |
| Revolution | 1800 rpm | |

4.2.4. Load Bank

The load bank is a forced air-cooled load bank with a rated capacity of 300 kW. It has high resistivity and experiences little change in resistance due to temperature increases. It uses an iron-chrome type 2 heating wire (FCHW-2). The load bank was used in the test bed to provide the electrical load for testing power sources, such as the generator or the uninterruptable power supply. The specifications

of the load bank are listed in Table 9. The resistance of the load bank was connected in parallel to allow the load capacity to be adjusted.

Table 9. Load bank specifications.

| Rated Capacity | | 300 kW | | | |
|--|----------|-------------------------|------------------|-----------------|-------------------------|
| Rated Voltage | | 3 Phase, 440 V, 60 Hz | | | |
| Current and Resistance Value for Each Capacity | | | | | |
| Unit Capacity (kW) | Quantity | Synthetic Capacity (kW) | Unit Current (A) | Unit Resistance | Enclosure Configuration |
| 0.1 | 1 | 0.1 | 0.13 | 1936 Ω | 1 box |
| 0.2 | 1 | 0.2 | 0.26 | 968 Ω | |
| 0.4 | 1 | 0.4 | 0.52 | 484 Ω | |
| 0.8 | 1 | 0.8 | 1.04 | 242 Ω | |
| 1 | 1 | 1 | 1.31 | 193.6 Ω | |
| 2 | 1 | 2 | 2.62 | 96.8 Ω | |
| 4 | 1 | 4 | 5.24 | 48.4 Ω | |
| 8 | 1 | 8 | 10.49 | 24.2 Ω | |
| 16 | 1 | 16 | 20.99 | 12.1 Ω | |
| 32 | 1 | 32 | 41.98 | 6.05 Ω | |
| 60 | 4 | 240 | 78.78 | 3.22 Ω | |
| Total | 15 | 304.5 | 399.7 | - | |

4.2.5. Intelligent Energy Management System (IEMS)

The intelligent energy management system (IEMS) is a control system which monitors the voltage, current, and output of each device and the system state in real time and enables the system to be operated reliably. It adjusts the load of the load bank according to the load pattern in real time and allows the different devices to be synchronized [42–46].

The test bed was organized such that the IEMS and power sources (MCFC, diesel generator system (DGS), and ESS) could send and receive device statuses and operation commands through an interface, as shown in Figure 6. Communications were based on an RS-285 and Ethernet to take into account noise and effects of external factors, such as surrounding devices. In addition, an external connection to the internet was used to allow the operating test bed system to be monitored from locations with internet connectivity.

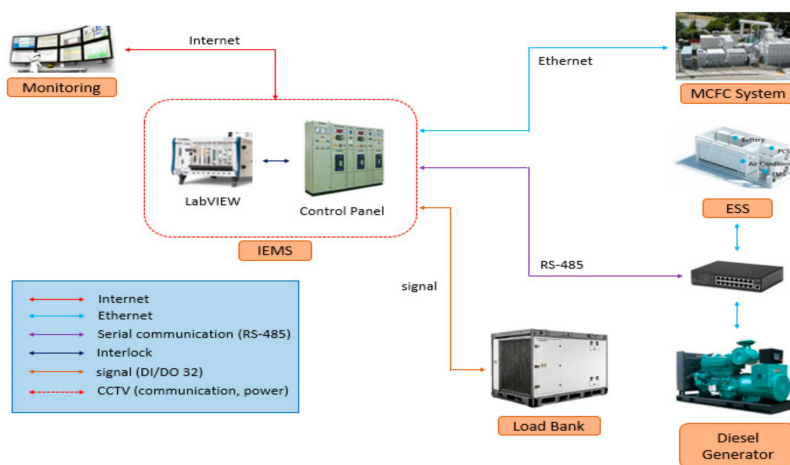


Figure 6. Diagram of interface design.

As shown in the Table 10 below, the control logic was configured to control the complex power system according to the SOC of the ESS according to the load.

Table 10. Configuration of control logic for power system.

| Load | | Control Condition |
|------------------------|---------------------|--|
| ≤100 kW | ESS SOC ≥ 80% | MCFC and Consumption Load leveler |
| | ESS SOC ≤ 80% | MCFC and Charging ESS |
| 101 kW ≤ Load ≤ 130 kW | ESS SOC ≥ 60% | MCFC and Charging ESS and Diesel Generator [D/G] Off |
| | 40% ≤ ESS SOC ≤ 60% | MCFC and ESS Discharging |
| | ESS SOC ≤ 40% | MCFC and ESS Discharging and D/G Operation |
| 131 kW ≤ Load ≤ 180 kW | ESS SOC ≤ 35% | MCFC and D/G Operation, ESS limit (≤20 kW) |
| | ESS SOC ≤ 30% | MCFC and D/G Operation, ESS limit (≤10 kW) |
| | ESS SOC ≤ 25% | MCFC and D/G Operation, ESS off |

4.3. Comparison of Fuel Consumption and CO₂ Emission Reduction Rates of the Conventional Commercial Diesel Engine vs. the Hybrid Power Source

4.3.1. Conventional Commercial Diesel Power Source vs. the Fuel-Cell-Based Hybrid Power Source (FCHPS)

The conventional commercial diesel power source was selected from the Doosan Infracore’s P126-TI model with a capacity of 241 kW, which was optimized for an average load of 80%. This generator’s specific rated power was 80% load of 241 kW, 192.8 kW and selected as the standard model of the diesel generator of the test bed. The diesel generator for fuel cell-based hybrid power source was selected as a DB-58 model with a capacity of 70 kW among the diesel engines of the Doosan Infracore’s generator. The generator was also optimized for an average load of 80%, 56 kW was selected as the diesel generator reference model for the combined power source of the test bed.

In order to analyze the CO₂ emissions reduction of the combined power source, the fuel consumption and the carbon dioxide emissions of the commercial diesel generator optimized for the same power as the hybrid power source were applied to the baseload. To compare the fuel consumption of the MCFC and the diesel generator of the combined power source, each fuel consumption amount was converted into the petroleum conversion factor (1 Tonnage of oil equivalent [TOE] = 1000 kgoe). As shown in the Tables 11 and 12, the fuel consumption factor of the diesel generator and the MCFC were matched by applying the energy calorific value conversion factor to each fuel consumption amount for application of the petroleum conversion factor.

Table 11. Flow conversion formula and CO₂ emission calculation formula.

| Power Source | Calculation Method of Fuel Consumption | Calculation Method of CO ₂ |
|------------------|---|---|
| Diesel generator | Kgoe/h = flow (L/h) × 0.901 | CO ₂ = 0.857 × flow (L/h) × (3.206 + 0.3 + 0.08) |
| Fuel cell | Kgoe/h = flow (m ³ /h) × 1.043 | CO ₂ = 0.631 × Electric Energy (kWh) |

Table 12. Conversion standard of energy calorific value.

| Fuel | Unit | Gross Calorific Value | | | Net Calorific Value | | |
|--------|-----------------|-----------------------|--------|----------------------|---------------------|------|----------------------|
| | | MJ | kcal | 10 ⁻³ TOE | MJ | kcal | 10 ⁻³ TOE |
| Diesel | L | 37.7 | 9010 | 0.901 | 35.2 | 8420 | 0.842 |
| LNG | Nm ³ | 43.6 | 10,430 | 1.043 | 39.4 | 9420 | 0.942 |

Estimation of greenhouse gas emissions was based on the methodology presented in the IPCC Guidelines. In international organizations and countries, emission factors are calculated and used according to the IPCC Guidelines. IMO has also developed a method for estimating carbon dioxide emissions for ships based on the IPCC Guidelines. However, the IPCC Guidelines provide a methodology for estimating emission factors, but IMO suggests a calculation method using conversion factors [47]. Tables 11 and 12 show a calculation formula and conversion standard.

4.3.2. Analysis of Fuel Consumption and CO₂ Emissions Reduction in Hybrid Power Source

The test bed used in this study consisted of a hybrid power source with a combined capacity of 180 kW (100 kW fuel cell, 30 kW battery, and 50 kW diesel generator). The power generation in the hybrid power source was designed such that the fuel cell was set for base-load operation and the battery and diesel generator operated in sequence. At 100 kW in Figure 7, there is a 1% difference in the fuel consumption of the commercial diesel generator and the fuel cell. At 130 kW, the difference in fuel consumption with the diesel generator increases because the fuel cell and the battery, which does not need fuel supply, are operating. At 180 kW, the fuel cell, battery, and diesel generator were operating, and it can be seen that there was a reduction in the fuel consumption and CO₂ emissions of the hybrid power source compared to the commercial diesel generator. At 100 kW in Figure 8, the CO₂ emissions of the fuel cell are 9% of those of the commercial diesel engine. At 130 kW, at which the fuel cell and battery were operating, the difference in CO₂ emissions compared with the diesel generator increases. At 180 kW, at which the fuel cell, battery, and diesel generator were operating, the CO₂ emissions of the hybrid power source were reduced by 39% compared to that of the commercial diesel generator. Table 13 shows the CO₂ emission reduction rates.

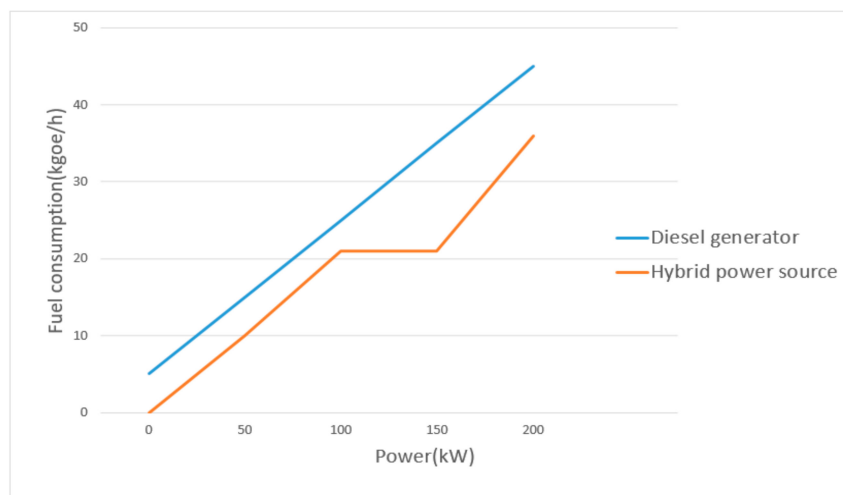


Figure 7. Comparison of fuel consumption of the commercial diesel generator and the hybrid power source.

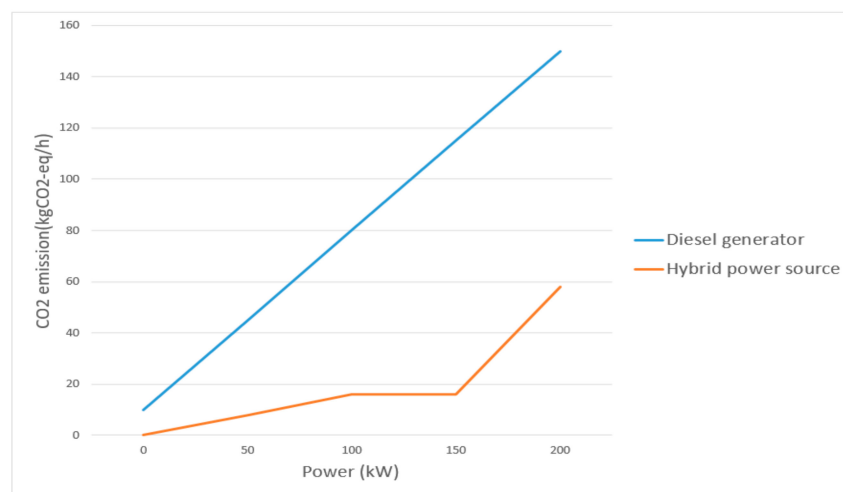


Figure 8. Comparison of CO₂ emissions of the commercial diesel generator and the hybrid power source.

Table 13. CO₂ emission reduction rates in the commercial diesel generator vs. the hybrid power source.

| | Fuel Consumption (kgoe/h) | CO ₂ Emissions (kgCO ₂ /h) |
|--------------------------------|---------------------------|--|
| Diesel generator | 43.5 | 148.5 |
| Hybrid power source | 35.6 | 57.7 |
| CO ₂ reduction rate | 61% | |

5. Analysis of Fuel Consumption and CO₂ Emission Reduction in a Fuel-Cell-Based Hybrid Power Source Using Simulations of Operating Profiles by Type of Ship

The actual electric load analysis values that were used in this study were taken from the operating profiles of ships, including a 5500 TEU Reefer Container, a 13000 TEU Container, a 40 k DWT Bulk Carrier, 130 k DWT LNG Carrier, and 300 k DWT very large crude oil carrier (VLCC). These values were scaled down for each operation mode and suitable load scenarios for each ship type were used. To utilize scale-down methodology, the linear interpolation method is applied [48]. For example, if the original 5500 TEU Reefer Container’s rated power is 4154 kW, the rated power of the test bed is 180 kW, when applying the scale down method. At part load, 1424 kW will be converted to 61 kW. All following test bed operating loads were calculated in this way. For the load scenarios in Table 14, according to the ship type operating scenarios, the following power sources were applied.

Table 14. Load scenario according to the ship type.

| Vessels | Operation Mode | Power Sources |
|---------------------------|------------------------------|---------------------------|
| 5500 TEU Reefer Container | Normal seagoing (w/o reefer) | Fuel Cell |
| | Normal seagoing (w/reefer) | Fuel Cell + Battery + D/G |
| | Port in/out (w/o thruster) | Fuel Cell |
| | Port in/out (w/ thruster) | Fuel Cell + Battery + D/G |
| | Load/Unload | Fuel Cell + Battery + D/G |
| 13,000 TEU Container | Normal seagoing | Fuel Cell |
| | Port in/out (w/o thruster) | Fuel Cell + Battery |
| | Port in/out (w/ thruster) | Fuel Cell + Battery + D/G |
| | Load/Unload | Fuel Cell |
| 40 k DWT Bulk Carrier | Harboring | Fuel Cell |
| | Normal seagoing | Fuel Cell |
| | Port in/out | Fuel Cell + Battery + D/G |
| | Loading (shore crane) | Fuel Cell + Battery |
| 130 k DWT LNG Carrier | Loading (crane) | Fuel Cell + Battery + D/G |
| | Harboring | Fuel Cell |
| | Normal seagoing | Fuel Cell |
| | Port in/out | Fuel Cell + Battery + D/G |
| | Port discharging | Fuel Cell + Battery + D/G |
| 300 k DWT VLCC | Port loading | Fuel Cell + Battery + D/G |
| | Port idle gas free | Fuel Cell |
| | Normal seagoing | Fuel Cell |
| | W/I.G.S Topping up | Fuel Cell + Battery |
| | Tank cleaning | Fuel Cell + Battery + D/G |
| 300 k DWT VLCC | Port in/out | Fuel Cell + Battery + D/G |
| | Load/Unload | Fuel Cell + Battery + D/G |

5.1. 5500 TEU Reefer Container

The 5500 TEU reefer container uses the following operating modes during operations: Normal seagoing (without reefer), normal seagoing (with reefer), port in/out (without thruster), port in/out (with thruster), and load/unload. To perform the test bed experiments, the scale of the values obtained as a result of the electric load analysis were adjusted to reflect the output of each operating mode of an

actual ship. As shown in Figure 9, the hybrid power source was used in the load scenarios of this ship. Normal seagoing (without reefer) was a fuel cell operation interval. Normal seagoing (with reefer) was a fuel cell + battery + diesel generator operation interval. Port in/out (without thruster) was a fuel cell operation interval. Port in/out (with thruster) and load/unload were fuel cell + battery + diesel generator operation intervals. The scale-adjusted electric load analysis was applied to the test bed, and the output tests were carried out.

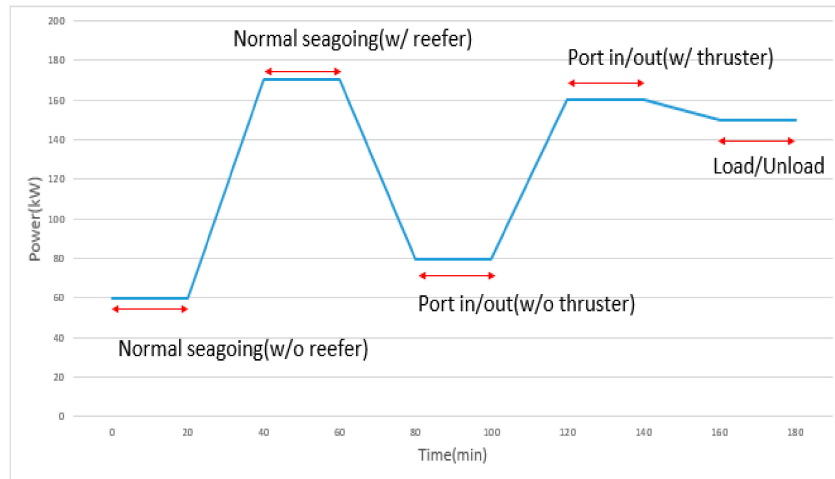


Figure 9. Power consumption of 5500 TEU reefer container during different operation modes.

Figure 10 compares the fuel consumption during each operating mode of this ship. The fuel consumption reached a maximum during the normal seagoing (with reefer) mode and a minimum during the normal seagoing (without reefer) mode. As the load increased, the fuel consumption increased; similarly, as the load decreased, the fuel consumption decreased. However, when observing the CO₂ emission reduction rates shown in Figure 11, it can be seen that the CO₂ emission reduction rate was the highest in the port in/out (without thruster) mode, during which the second least amount of fuel was consumed.

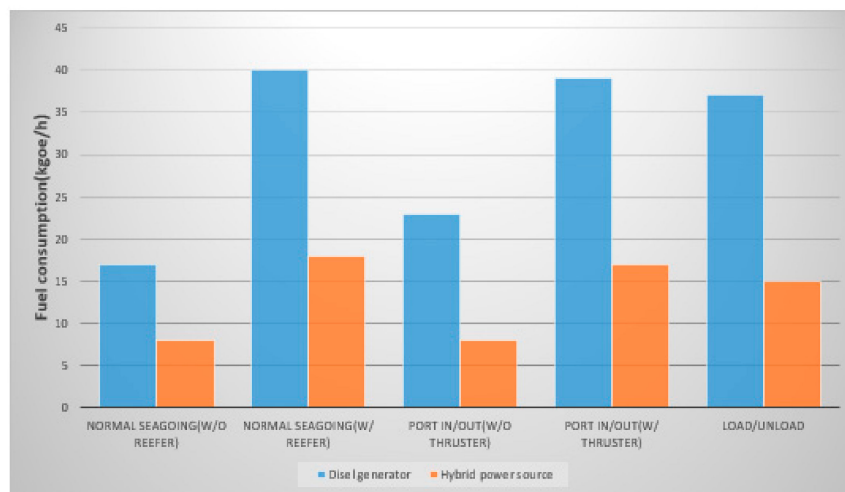


Figure 10. Fuel consumption in each operating mode of the 5500 TEU reefer container.

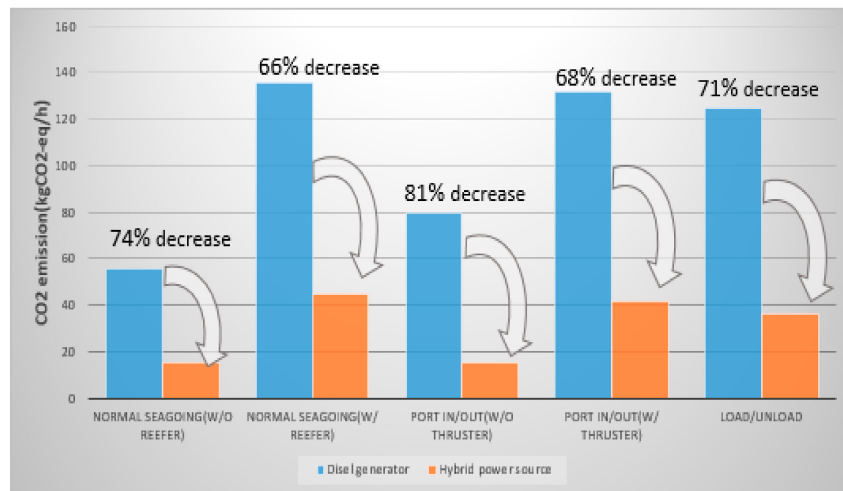


Figure 11. Comparison of CO₂ emissions and CO₂ emission reduction rate in each operating mode of the 5500 TEU reefer container.

5.2. 13000 TEU Container

The 13000 TEU container uses the following operating modes during voyage: Normal seagoing, port in/out (without thruster), port in/out (with thruster), load/unload, and harboring. The test bed experiments were conducted by adjusting the scale of the values obtained from the electric load analysis or the output of each operating mode of an actual ship. As shown in Figure 12, the hybrid power source was used in the load scenarios of this ship. Normal seagoing was a fuel cell operation interval. Port in/out (without thruster) was a fuel cell + battery operation interval. Port in/out (with thruster) was a fuel cell + battery + diesel generator operation interval. Load/unload and harboring were fuel cell operation intervals. The scale-adjusted electric load analysis was applied to the test bed, and the output tests were performed.

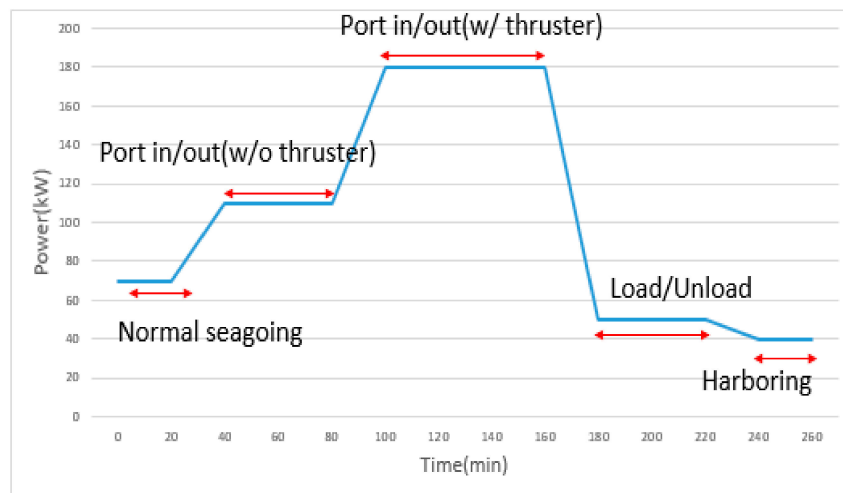


Figure 12. Operating modes of the 13000 TEU container.

Figure 13 compares the fuel consumption during each operating mode of this ship. The fuel consumption was at maximum during the port in/out (with thruster) mode and at minimum during the load/unload mode. The load increased (and decreased) as the fuel consumption increased (and decreased), respectively. However, on observing the CO₂ emission reduction rates shown in Figure 14, it can be seen that the CO₂ emission reduction rate was low in the load/unload and harboring modes despite the low fuel consumption.

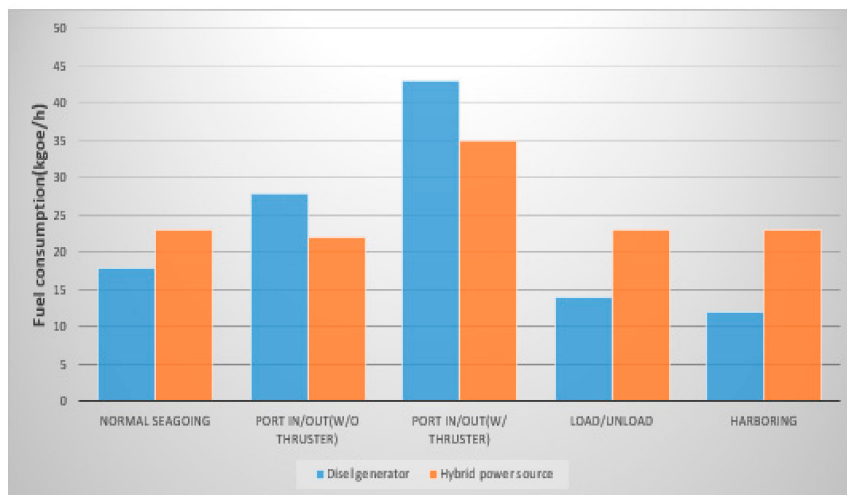


Figure 13. Fuel consumption in each operating mode of the 13000 TEU container ship.

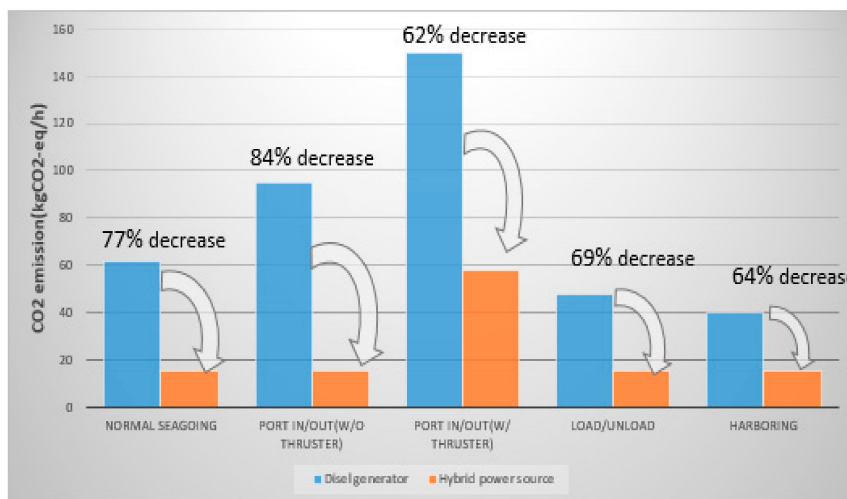


Figure 14. Comparison of CO₂ emissions and CO₂ emission reduction rate in each operating mode of the 13000 TEU container ship.

5.3. 40 k DWT Bulk Carrier

The 40 k DWT bulk carrier uses the following operating modes during operations: Normal seagoing, port in/out, loading (shore crane), loading (deck crane), and harboring. To perform the test bed experiments, the scale of the values obtained as a result of the electric load analysis was adjusted according to the output of each operating mode of an actual ship. As shown in Figure 15, the hybrid power source was used in the load scenarios. Normal seagoing was a fuel cell operation interval. Port in/out was a fuel cell + battery + diesel generator operation interval. Port in/out (with thruster) was a fuel cell + battery + diesel generator operation interval. Loading (shore crane) was a fuel cell + battery operation interval. Loading (deck crane) was a fuel cell + battery + diesel generator operation interval. Harboring was a fuel cell interval. The scale-adjusted electric load analysis was applied to the test bed before the output tests were performed.

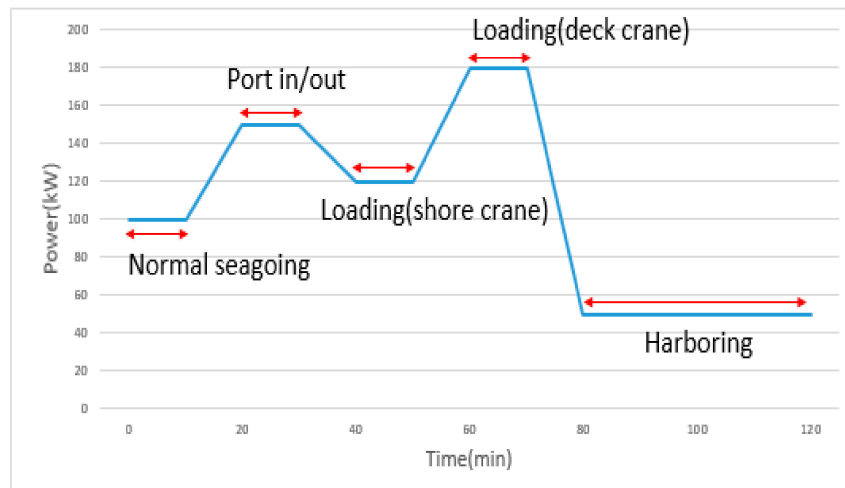


Figure 15. Operating modes of the 40 k DWT bulk carrier.

Figure 16 compares the fuel consumption during each operating mode of this ship. The fuel consumption was at maximum during the loading (deck crane) mode and at minimum during the harboring mode. The fuel consumption increased as the load increased, and decreased as the load decreased. However, on observing the CO₂ emission reduction rates shown in Figure 17, it can be seen that the CO₂ emission reduction rate of the loading (shore crane) mode was as high as 85% even though this operation consumed more fuel than during normal seagoing operations.

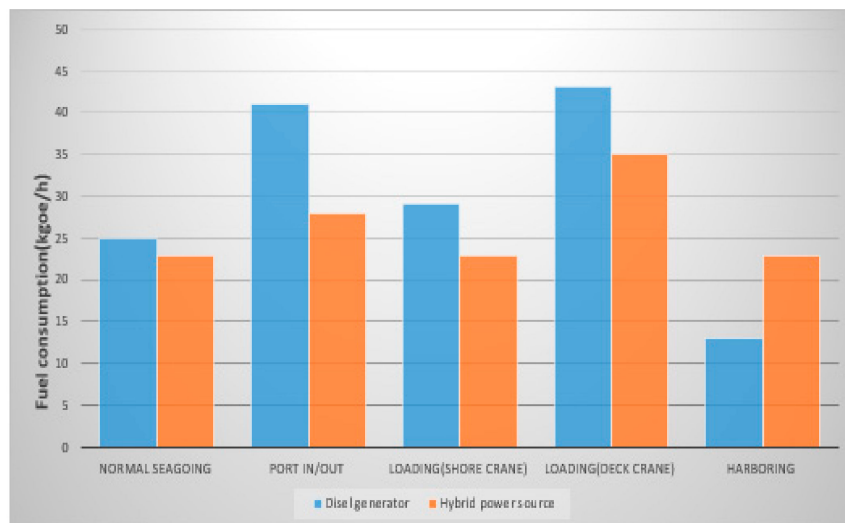


Figure 16. Fuel consumption in each operating mode of the 40 k DWT bulk carrier.

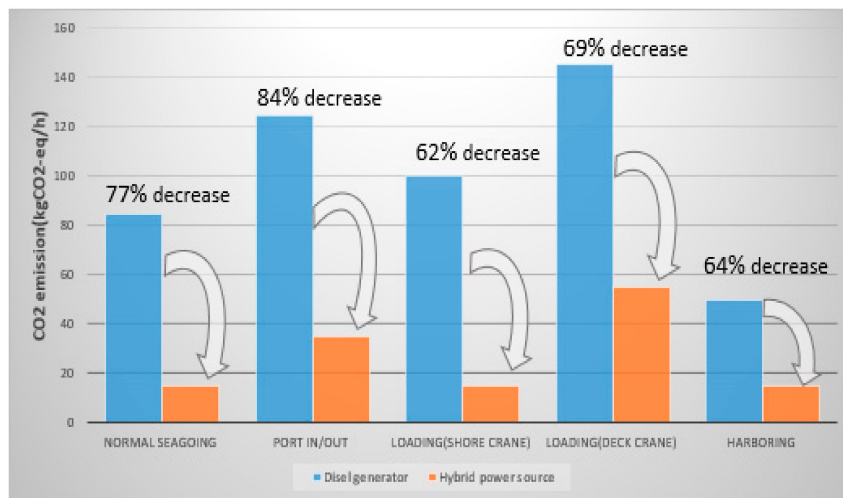


Figure 17. Comparison of CO₂ emissions and CO₂ emission reduction rate in each operating mode of the 40 k DWT bulk carrier.

5.4. 130 k DWT LNG Carrier

The 130 k DWT LNG carrier uses the following operating modes during its operations: Normal seagoing, port in/out, port discharging, port loading, and port idle gas free. The test bed experiments were conducted by adjusting the scale of the values obtained from the electric load analysis based on the output of each operating mode of an actual ship. As shown in Figure 18, the hybrid power source was used in the load scenarios of this ship. Normal seagoing was a fuel cell operation interval. Port in/out, port discharging, and port loading were fuel cell + battery + diesel generator operation intervals. Port idle gas free was a fuel cell operation interval. The scale-adjusted electric load analysis was applied to the test bed, and the output tests were performed.

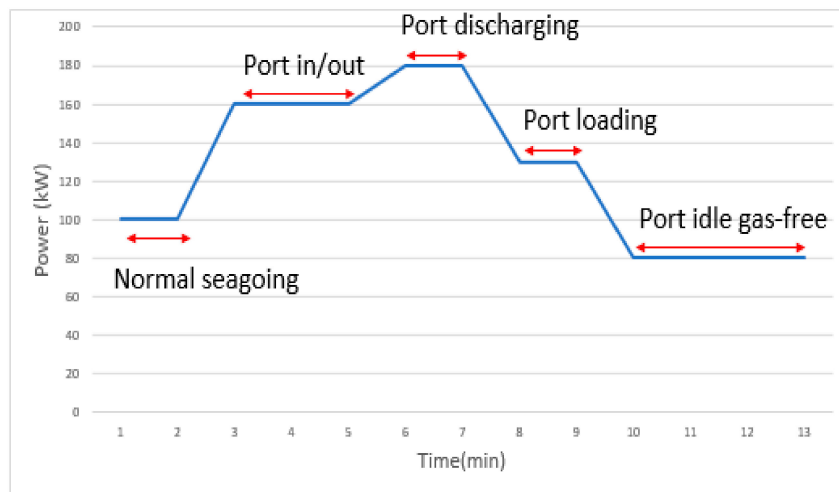


Figure 18. Operating modes of the 130 k DWT LNG carrier.

Figure 19 compares the fuel consumption during each operating mode of this ship. The maximum amount of fuel was consumed during the port discharging mode, whereas it reached a minimum during the port idle gas free mode. The fuel consumption increased and decreased as the load increased and decreased, respectively. However, on examining the CO₂ emission reduction rates shown in Figure 20, it can be seen that the CO₂ emission reduction rate of the normal seagoing mode was as high as 83%, even though the fuel consumption in this mode exceeded that in the port idle gas free mode.

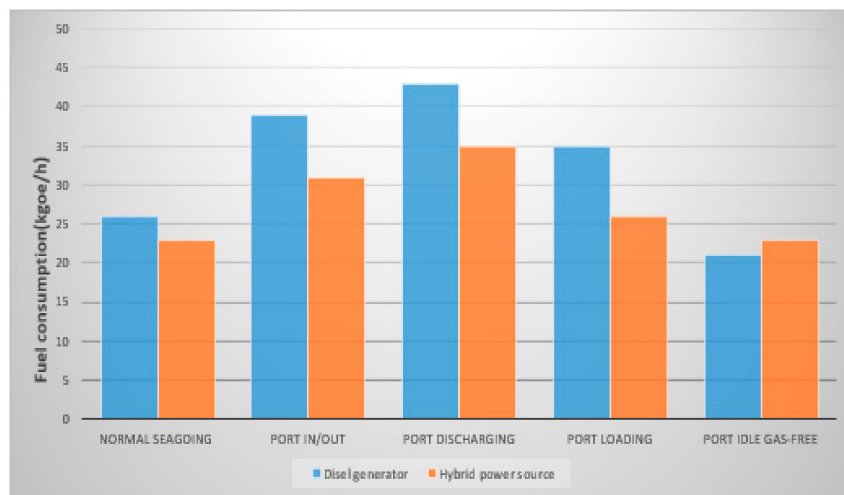


Figure 19. Fuel consumption in each operation mode of the 130k DWT LNG carrier.

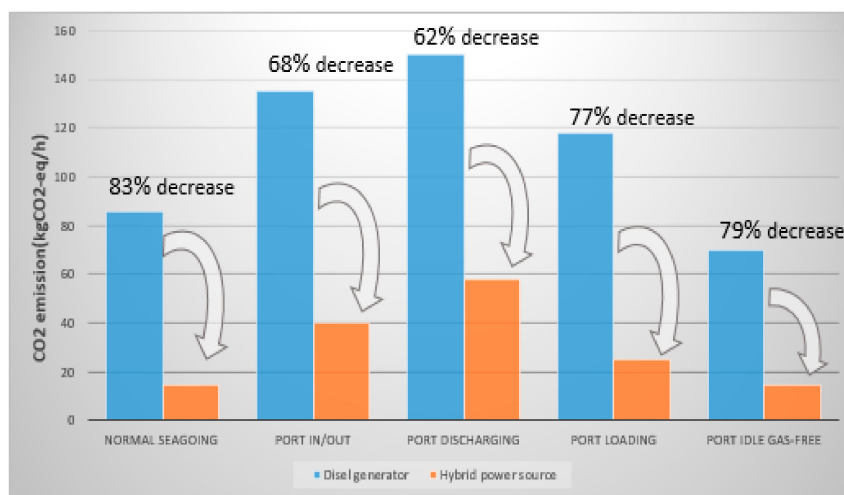


Figure 20. Comparison of CO₂ emissions and CO₂ emission reduction rate in each operating mode of the 130 k DWT LNG carrier.

5.5. 300 k DWT Very Large Crude Oil Carrier (VLCC)

The 300 k DWT VLCC uses the following operating modes during operations: Normal seagoing, with an inert gas supply system (IGS) topping up, tank cleaning, port in/out, and load/unload. An adjustment was made to the scale of the values of the electric load analysis of the output of each operating mode of an actual ship to perform the test bed experiments. As shown in Figure 21, the hybrid power source was used in the load scenarios of this ship. Normal seagoing was a fuel cell operation interval. With IGS topping up was a fuel cell + battery operation interval. Tank cleaning, port in/out, and load/unload were fuel cell + battery + diesel generator operation intervals. The scale-adjusted electric load analysis was applied to the test bed, and the output tests were performed.

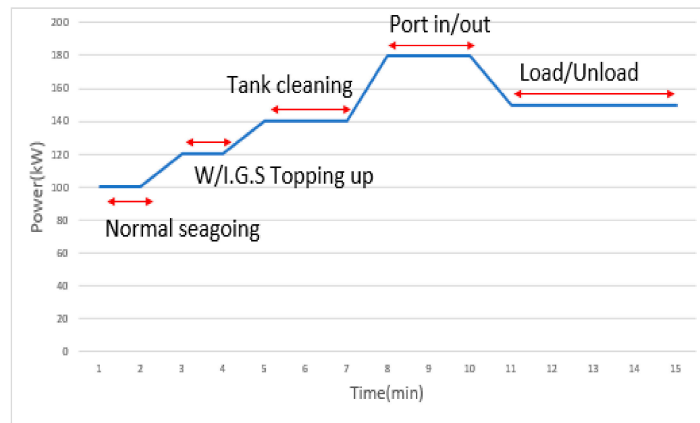


Figure 21. Operating modes of the 300 k DWT VLCC.

Figure 22 compares the fuel consumption during each operating mode of this ship. The fuel consumption was at maximum during the port in/out mode and at minimum during the normal seagoing mode. The fuel consumption increased as the load increased and decreased as the load decreased. However, on observing the CO₂ emission reduction rates shown in Figure 23, it can be seen that the CO₂ emission reduction rate in the IGS topping up mode was as high as 85%, even though the fuel consumption in this mode was higher than in normal seagoing mode.

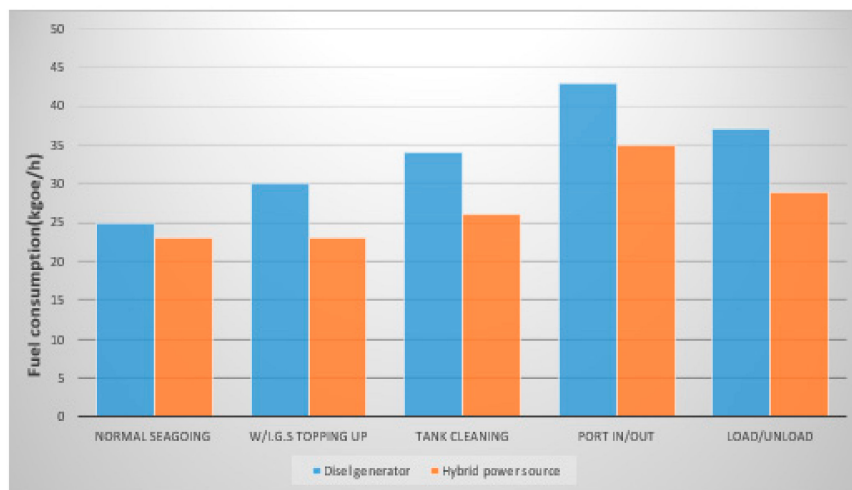


Figure 22. Fuel consumption in each operating mode of the 300 k DWT VLCC.

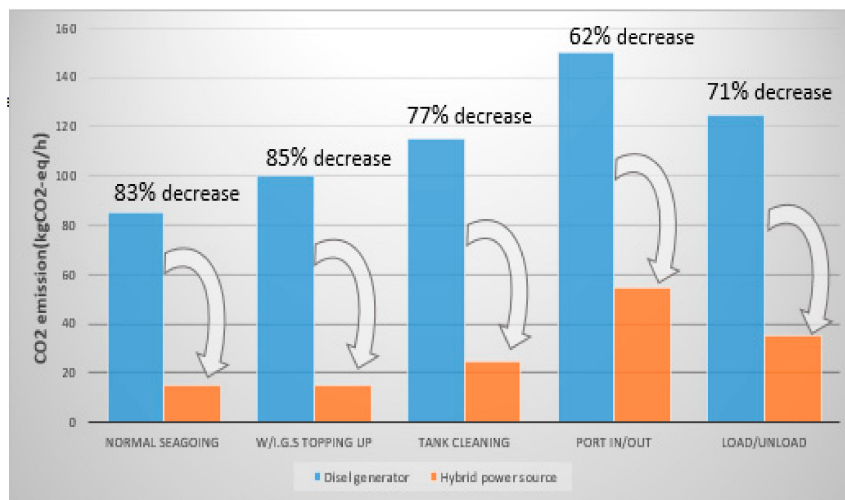


Figure 23. Comparison of CO₂ emissions and CO₂ emission reduction rate in each operating mode of the 300 k DWT VLCC.

Operating profile scenarios for each type of ship were developed, and the five developed load scenarios were applied to the test bed. The results are presented in Table 15.

Table 15. Cumulative CO₂ emissions and reductions at load scenario.

| Case | CO ₂ Emissions (kgCO ₂) | | Fuel Consumption (kgoe) | | CO ₂ Reduction Rate | Experiment Time (h:m:s) |
|---------------------------|--|---------------------|-------------------------|---------------------|--------------------------------|-------------------------|
| | Diesel Generator | Hybrid Power Source | Diesel Generator | Hybrid Power Source | | |
| 5500 TEU Reefer Container | 205.6 | 56.8 | 60.3 | 54.1 | 72 | 2:50:59 |
| 13,000 Container | 233.9 | 69.5 | 68.6 | 57.8 | 70 | 4:01:01 |
| 40 k DWT Bulk Carrier | 184.9 | 49.8 | 54.2 | 52.0 | 73 | 2:01:07 |
| 130 k DWT LNG Carrier | 217.7 | 59.6 | 63.8 | 54.9 | 73 | 2:00:23 |
| 300 k DWT VLCC | 238.5 | 62.8 | 69.9 | 55.8 | 74 | 2:00:20 |

6. Conclusions

This study analyzed the fuel consumption and CO₂ emission reduction rates when a fuel-cell-based hybrid power source instead of a conventional commercial diesel power source was used in ships. The results showed that under the rated output on a test bed with a load bank of 180 kW, the conventional commercial diesel generator consumed fuel at 43.5 kgoe/h and emitted CO₂ at 148.5 kg/h, whereas the fuel-cell-based hybrid power source consumed fuel at 35.6 kgoe/h and emitted CO₂ at 57.7 kg/h, as given in Table 11. The hybrid power source reduced fuel consumption by 18% and CO₂ emissions by 61% at part load in the port period. These results indicate that it is possible to reduce CO₂ emissions by up to 61% if a hybrid power source of the same capacity is used to power a ship.

In this study, the actual electric load analysis values of the 5500 TEU Reefer Container, 13 k TEU Container, 40 k Bulk Carrier, 130 k DWT LNG Carrier, and 300 k DWT Crude Oil Tanker were scaled down according to the operation mode, and the control logic and systems of the test bed developed in

this study were operated normally according to the respective load scenarios. The experimental results of applying the developed five load scenarios to the test bed are shown in Table 15.

Because the output characteristics and control time of the diesel generator, according to the power source of the hybrid system, were reduced, according to the load variation pattern of the ship and the ship's type, the CO₂ emissions of the hybrid system, as compared with the case of the diesel generator, alone operated for each load scenario with an average of 70%~74% less.

In order to apply the hybrid system to ships, it is possible to maximize the CO₂ emission reduction effect by setting the capacity of the fuel cell + battery to be able to take charge of the base load of the ship through analysis of the base load of each ship type.

Author Contributions: Conceptualization, G.R., H.K. and K.Y.; Methodology, G.R., K.Y. and H.J.; Formal analysis, G.R. and H.J.; Supervision, H.K. and K.Y., Visualization, H.J; Writing-original draft preparation, G.R. and K.Y.; Writing-review and editing, K.Y.

Funding: This research received no external funding.

Acknowledgments: We thank our colleagues from Jong Su Kim who provided insight and expertise that greatly assisted the research, although they may not agree with all of the conclusions of this paper.

Conflicts of Interest: The authors declare no conflicts of interest.

Nomenclature

| | |
|--------|--|
| AFC | Alkaline fuel cell |
| DWT | Deadweight tons |
| EBOP | Electric balance of plant |
| EEDI | Energy efficiency design index |
| EPSS | Electric power switching system |
| ESS | Energy storage system |
| IEMS | Intelligent energy management system |
| IGS | Inert gas system |
| IMO | International maritime organization |
| IPCC | Intergovernmental panel on climate change |
| KGOE | Kilograms of oil equivalent |
| MARPOL | The international convention for the prevention of marine pollution from ships |
| MCFC | Molten carbonate fuel cell |
| MDOP | Machinery balance of plant |
| PAFC | Phosphoric acid fuel cells |
| PCS | Power conditioning system |
| PEMFC | Polymer electrolyte membrane fuel cell |
| PFD | Process flow diagram |
| PM | Particulate matter |
| SFC | Specific fuel consumption |
| SOC | State of charge |
| SOFC | Solid oxide fuel cell |
| TEU | Twenty-foot equivalent units |
| VLCC | Very large crude-oil carrier |

References

1. International Maritime Organization. Third IMO Greenhouse Gas Study. Available online: <http://www.imo.org/en/OurWork/Environment/PollutionPrevention/AirPollution/Documents/Third%20Greenhouse%20Gas%20Study/GHG3%20Executive%20Summary.pdf> (accessed on 15 August 2015).
2. Bouman, E.A.; Lindstad, E.; Riialand, A.I.; Strømman, A.H.; Lindstad, H.E. State-of-the-art technologies, measures, and potential for reducing GHG emissions from shipping—A review. *Transp. Res. Part D Transp. Environ.* **2017**, *52*, 408–421. [CrossRef]

3. European Parliament. Emission Reduction Targets for International Aviation and Shipping. Available online: [http://www.europarl.europa.eu/RegData/etudes/STUD/2015/569964/IPOL_STU\(2015\)569964_EN.pdf](http://www.europarl.europa.eu/RegData/etudes/STUD/2015/569964/IPOL_STU(2015)569964_EN.pdf) (accessed on 18 September 2015).
4. International Council on Clean Transportaion. Greenhouse Gas Emissions from Global Shipping. Available online: https://www.theicct.org/sites/default/files/publications/Global-shipping-GHG-emissions-2013-2015_ICCT-Report_17102017_vF.pdf (accessed on 1 October 2017).
5. International Maritime Organization. Marine Environment Protection Committee 72nd Session. Available online: <http://www.imo.org/en/MediaCentre/MeetingSummaries/MEPC/Pages/MEPC-72nd-session.aspx> (accessed on 13 April 2018).
6. Pestana, H. Future trends of electrical propulsion and implications to ship design. *Marit. Technol. Eng.* **2014**, *1*, 797–803.
7. Yang, Z.; Zhang, D.; Caglayan, O.; Jenkinson, I.; Bonsall, S.; Wang, J.; Huang, M.; Yan, X.; Yang, Z. Selection of techniques for reducing shipping NO_x and SO_x emissions. *Transp. Res. Part D Transp. Environ.* **2012**, *17*, 478–486. [[CrossRef](#)]
8. Sattler, G. Fuel Cells Going On-Board. *J. Power Sources* **2000**, *86*, 61–67. [[CrossRef](#)]
9. Tronstad, T.; Endresen, Ø. Fuel cells for low emission ships. In Proceedings of the International Renewable Energy Conference 2005, Beijing, China, 7–8 November 2005; pp. 141–149.
10. Schneider, J.; Dirk, S.; Schneider, J.; Dirk, S.; Motor, P. ZEMShip. In Proceedings of the 18th World Hydrogen Energy Conference 2010, Essen, Germany, 16–20 May 2010; Volume 78, pp. 132–135.
11. Yuan, J.; Ng, S.H.; Sou, W.S. Uncertainty quantification of CO₂ emission reduction for maritime shipping. *Energy Policy* **2016**, *88*, 113–130. [[CrossRef](#)]
12. Van Biert, L.; Godjevac, M.; Visser, K.; Aravind, P. A review of fuel cell systems for maritime applications. *J. Power Sources* **2016**, *327*, 345–364. [[CrossRef](#)]
13. De-Troya, J.J.; Álvarez, C.; Fernández-Garrido, C.; Carral, L. Analysing the possibilities of using fuel cells in ships. *Int. J. Hydrog. Energy* **2016**, *41*, 2853–2866. [[CrossRef](#)]
14. Andújar, J.; Segura, F.; Andujar-Márquez, J.M. Fuel cells: History and updating. A walk along two centuries. *Renew. Sustain. Energy Rev.* **2009**, *13*, 2309–2322. [[CrossRef](#)]
15. Inal, O.B.; Deniz, C. Fuel Cell Availability for Merchant Ships Fuel Cell Availability for Merchant Ships. In Proceedings of the 3rd International Symposium on Naval Architecture and Maritime (INT-NAM 2018), İstanbul, Turkey, 23–25 April 2018; Volume 1, pp. 907–916.
16. Tomczyk, P. MCFC versus other fuel cells—Characteristics, technologies and prospects. *J. Power Sources* **2006**, *160*, 858–862. [[CrossRef](#)]
17. Vogler, F.; Würsig, G. New Developments for Maritime Fuel Cell Systems. In Proceedings of the 18th World Hydrogen Energy Conference (WHEC 2010), Essen, Germany, 16–21 May 2010; Volume 78, pp. 444–453.
18. McConnell, V.P. Now, Voyager? The Increasing Marine Use of Fuel Cells. *Fuel Cells Bull.* **2010**, *2010*, 12–17. [[CrossRef](#)]
19. Tronstad, T.; Åstrand, H.H.; Haugom, G.P.; Langfeldt, L. *Study on the Use of Fuel Cells in Shipping*; EMSA European Maritime Safety Agency: Lisbon, Portugal, 2017; Volume 1, pp. 1–108.
20. Yazdanfar, J.; Mehrpooya, M.; Yousefi, H.; Palizdar, A. Energy and exergy analysis and optimal design of the hybrid molten carbonate fuel cell power plant and carbon dioxide capturing process. *Energy Convers. Manag.* **2015**, *98*, 15–27. [[CrossRef](#)]
21. Milewski, J.; Lewandowski, J.; Miller, A. Reducing CO₂ emissions from coal fired power plant by using a molten carbonate fuel cell. In Proceedings of the ASME Turbo Expo 2008, Berlin, Germany, 9–13 June 2008; pp. 1–7.
22. Welaya, Y.M.; El Gohary, M.M.; Ammar, N.R. A comparison between fuel cells and other alternatives for marine electric power generation. *Int. J. Nav. Arch. Ocean Eng.* **2011**, *3*, 141–149. [[CrossRef](#)]
23. Mekhilef, S.; Saidur, R.; Safari, A. Comparative study of different fuel cell technologies. *Renew. Sustain. Energy Rev.* **2012**, *16*, 981–989. [[CrossRef](#)]
24. Larminie, J.; Dicks, A. *Fuel Cell Systems Explained*; Wiley: Hoboken, NJ, USA, 2003.
25. International Maritime Organization. MARPOL Convention 73/78 Annex VI. Available online: [http://www.imo.org/en/About/Conventions/ListOfConventions/Pages/International-Convention-for-the-Prevention-of-Pollution-from-Ships-\(MARPOL\).aspx](http://www.imo.org/en/About/Conventions/ListOfConventions/Pages/International-Convention-for-the-Prevention-of-Pollution-from-Ships-(MARPOL).aspx) (accessed on 19 May 2005).

26. International Maritime Organization. IMO MEPC1/Circ 684. *Guidelines for Voluntary Use of the Ship Energy Efficiency Operational Indicator (EEOI)*. Available online: https://www.classnk.or.jp/hp/pdf/activities/statutory/eedi/mepc_1-circ_684.pdf (accessed on 17 August 2009).
27. International Maritime Organization. Ship Energy Efficiency Regulations and Related Guidelines. Available online: <http://www.imo.org/en/OurWork/Environment/PollutionPrevention/AirPollution/Documents/Air%20pollution/M2%20EE%20regulations%20and%20guidelines%20final.pdf> (accessed on 2 January 2016).
28. Woodyard, D. *Pounder's: Marine Diesel Engines and Gas Turbines*; Elsevier: Burlington, UK, 2004.
29. Zahedi, B.; Norum, L.E.; Ludvigsen, K.B. Optimized efficiency of all-electric ships by dc hybrid power systems. *J. Power Sources* **2014**, *255*, 341–354. [[CrossRef](#)]
30. Intergovernmental Panel on Climate Change. IPCC Guidelines for National Greenhouse Gas Inventories. Available online: <https://www.ipcc-nggip.iges.or.jp/public/2006gl/vol2.html> (accessed on 10 January 2006).
31. ISO. ISO 8271:2012 Petroleum Products—Specifications of Marine Fuels. Available online: <https://www.iso.org/obp/ui/#iso:std:iso:8217:ed-5:v1:en> (accessed on 5 March 2012).
32. International Maritime Organization. Marine Environment Protection Committee 65th Session Agenda Item 4. Available online: <http://yasinskiy.net/docs/wp-content/uploads/2018/06/MEPC.-65-INF.3-Rev.1.pdf> (accessed on 11 December 2012).
33. Park, S.-K.; Youn, Y.-M. Analysis of International Standardization Trend for the Application of Fuel Cell Systems on Ships. *J. Korean Soc. Mar. Environ. Saf.* **2015**, *20*, 579–585. [[CrossRef](#)]
34. Inci, M.; Türksoy, Ö. Review of fuel cells to grid interface: Configurations, technical challenges and trends. *J. Clean. Prod.* **2019**, *213*, 1353–1370. [[CrossRef](#)]
35. Kirubakaran, A.; Jain, S.; Nema, R. A review on fuel cell technologies and power electronic interface. *Renew. Sustain. Energy Rev.* **2009**, *13*, 2430–2440. [[CrossRef](#)]
36. Park, K.-D.; Roh, G.-T.; Kim, K.-H.; Ahn, J.-W. Experimental study on development of a marine hybrid power system. *J. Korean Soc. Mar. Eng.* **2017**, *41*, 495–500. [[CrossRef](#)]
37. Bassam, A.M.; Phillips, A.B.; Turnock, S.R.; Wilson, P.A. An improved energy management strategy for a hybrid fuel cell/battery passenger vessel. *Int. J. Hydrog. Energy* **2016**, *41*, 22453–22464. [[CrossRef](#)]
38. Fuel Cell Energy Inc. 300kW DFC300 Specification. Available online: http://www.fuelcellenergy.com/assets/PID000155_FCE_DFC300_r1_hires.pdf (accessed on 16 August 2011).
39. Milewski, J.; Świercz, T.; Badyda, K.; Miller, A.; Dmowski, A.; Biczal, P. The control strategy for a molten carbonate fuel cell hybrid system. *Int. J. Hydrog. Energy* **2010**, *35*, 2997–3000. [[CrossRef](#)]
40. Heidebrecht, P.; Sundmacher, K. Molten carbonate fuel cell (MCFC) with internal reforming: Model-based analysis of cell dynamics. *Chem. Eng. Sci.* **2003**, *58*, 1029–1036. [[CrossRef](#)]
41. Cao, J.; Emadi, A. A New Battery/Ultracapacitor Hybrid Energy Storage System for Electric, Hybrid, and Plug-in Hybrid Electric Vehicles. *IEEE Trans. Power Electron.* **2012**, *27*, 122–132.
42. Choi, C.H.; Yu, S.; Han, I.-S.; Kho, B.-K.; Kang, D.-G.; Lee, H.Y.; Seo, M.-S.; Kong, J.-W.; Kim, G.; Ahn, J.-W.; et al. Development and demonstration of PEM fuel-cell-battery hybrid system for propulsion of tourist boat. *Int. J. Hydrog. Energy* **2016**, *41*, 3591–3599. [[CrossRef](#)]
43. Han, J.; Charpentier, J.-F.; Tang, T. An Energy Management System of a Fuel Cell/Battery Hybrid Boat. *Energies* **2014**, *7*, 2799–2820. [[CrossRef](#)]
44. San Martín, J.L.; Zamora, I.; Asensio, F.J.; García Villalobos, J.; San Martín, J.J.; Aperribay, V. Control and Management of a Fuel Cell Microgrid. Energy Efficiency Optimization. *Renew. Energy Power Qual. J.* **2017**, *7*, 314–319. [[CrossRef](#)]
45. Garcia, P.; Fernandez, L.M.; Garcia, C.A.; Jurado, F.; Fernández-Ramirez, L.M. Energy Management System of Fuel-Cell-Battery Hybrid Tramway. *IEEE Trans. Ind. Electron.* **2010**, *57*, 4013–4023. [[CrossRef](#)]
46. Jabir, M.; Mokhlis, H.; Muhammad, M.A.; Illias, H.A. Optimal battery and fuel cell operation for energy management strategy in MG. *IET Gener. Transm. Distrib.* **2019**, *13*, 997–1004. [[CrossRef](#)]

47. National Law Information Center of Korea. Enforcement Rule of Energy Law. Available online: <http://law.go.kr/nwRvsLsInfoR.do?lsiSeq=200561> (accessed on 28 December 2017).
48. Ha, Y.-J.; Lee, Y.-G.; Kang, B.H. A Study on the Estimation of the Form Factor of Full-Scale Ship by the Experimental Data of Geosim Models. *J. Soc. Nav. Arch. Korea* **2013**, *50*, 291–297. [[CrossRef](#)]



© 2019 by the authors. Licensee MDPI, Basel, Switzerland. This article is an open access article distributed under the terms and conditions of the Creative Commons Attribution (CC BY) license (<http://creativecommons.org/licenses/by/4.0/>).